

Chaotic provinces in the kingdom of the Red Queen

Hanna Schenk¹, Arne Traulsen¹ and Chaitanya S. Gokhale^{1,2,*}

¹Department of Evolutionary Theory, Max Planck Institute for Evolutionary Biology,
August-Thienemann Str-2, 24306 Plön, Germany

²New Zealand Institute for Advanced Study, Massey University, Albany, Private Bag 102904
North Shore Mail Centre, 0745, Auckland, New Zealand

*gokhale@evolbio.mpg.de, Tel: + 49 4522 763-269, Fax: +49 4522 763-260

Running title: Host-Parasite coevolution with multiple types

Abstract

The interplay between parasites and their hosts is found in all kinds of species and plays an important role in understanding the principles of evolution and coevolution. Usually, the different genotypes of hosts and parasites oscillate in their abundances. The well-established theory of oscillatory Red Queen dynamics proposes an ongoing change in frequencies of the different types within each species. So far, it is unclear in which way Red Queen dynamics persists with more than two types of hosts and parasites. In our analysis, an arbitrary number of types within two species are examined in a deterministic framework with constant or changing population size. This general framework allows for analytical solutions for internal fixed points and their stability. For more than two species, apparently chaotic dynamics has been reported. Here we show that even for two species, once more than two types are considered per species, irregular dynamics in their frequencies can be observed in the long run. The nature of the dynamics depends strongly on the initial configuration of the system; the usual regular Red Queen oscillations are only observed in some parts of the parameter region.

Keywords: coevolution, multiple types, mathematical model, population size, stability, Red Queen, chaos

1 Introduction

Studying host-parasite coevolution using mathematical models has lead to substantial advances in our understanding of the dynamics of the interaction. For example hypothesising the role of reciprocal selection between the antagonistic species in the evolution of virulence and tolerance. We specifically focus on the Red Queen hypothesis (van Valen, 1973; Stenseth and Maynard Smith, 1984; Dieckmann et al., 1995; Clay and Kover, 1996; Salathé et al., 2008). The hypothesis has been used in a broad context, leading to multiple definitions (Brockhurst et al., 2014; Rabajante et al., 2015). According to Van Valen, the maintenance of biodiversity is possible as long as the species displace each other, or when the resource distribution changes over time (van Valen, 1973). However, the different definitions are underlined by the presence of the typical dynamics expected within a species, namely Red Queen oscillations. These oscillations imply an interaction where the increase in the relative abundance of a certain type within a species indicates an equal decrease in relative abundance of another type (Maynard Smith, 1976; Van Valen, 1977). In the context of hosts and parasites, indications for such oscillations in densities have been empirically confirmed for e.g. in dormant stages of the water flea *Daphnia magna* from pond sediments (Decaestecker et al., 2007) and freshwater snails *Potamopyrgus antipodarum* (Koskella and Lively, 2009). However, while it is already difficult to analyse these dynamics experimentally over a single cycle, the long term dynamics of such systems is challenging.

The co-evolution of hosts and parasites has for example been used to explain sexual reproduction (Lively, 2010). However, when multilocus genetics is at play, features of co-evolution models, such as the maintenance of polymorphism and evolution of sex, depend on the exact interactions patterns (Frank, 1993a; Parker, 1996; Frank, 1996; Sasaki, 2000; Metzger et al., 2016). Exploring a variety of interaction patterns between multiple types of hosts and parasites, we show that short-term oscillations as the ones observed experimentally can be recovered in virtually all of these models, but one has to be very careful in extrapolating this kind of dynamics over a wider time horizon.

Mathematical models of host-parasite interactions with two types have been extensively anal-

ysed. A specific experiment in *Daphnia magna* (Carius et al., 2001) showed considerable variation in hosts (susceptibility) and parasites (infectiousness) of nine distinct types, which illustrates the necessity of considering models with more than two types. A recent model (Rabajante et al., 2015) based on ordinary differential equations numerically explored different numbers of types. The result strengthened the theory of the oscillatory Red Queen dynamics. In such numerical models, a broader exploration of the parameter space can lead to more general results and show the robustness of models. Here, we take a different approach and ask how complicated a model can become before the regular frequency dependent oscillations are lost? To tackle this question, we used analytical tools in addition to numerical integration.

Another aspect to be considered is the impact of population size (Papkou et al., 2016): A host population suffering from intense parasite pressure should decrease in absolute size. Similarly, a parasite population not finding sufficient hosts should decrease in absolute size. Recently, the impact of such changing population sizes was studied for two types (Gokhale et al., 2013; Song et al., 2015), including matching alleles (Frank, 1993b) or the gene-for-gene type of interactions (Flor, 1955; Engelstädter, 2015; Agrawal and Lively, 2002). By adjusting the birth rates of hosts and death rates of parasites to include frequency dependence, we can impose a constant population size. Such a transformation makes the underlying model identical to replicator dynamics (Taylor and Jonker, 1978; Hofbauer and Sigmund, 1998; Schuster and Sigmund, 1983).

Here, we extend the two approaches with changing and constant population size to an arbitrary number of types of hosts and parasites. As a simple example, we first consider the matching allele model: Each host can only be infected by its specific parasite type, and each parasite can only affect the one matching host. Next, cross-infectivity is incorporated so that two genetically similar parasites (neighbours to the focal parasite) can additionally infect a particular host in an equally robust manner and vice versa: each parasite can infect not only one host but also two more closely related hosts. Finally, a general model where different infectivity magnitudes are realised for each parasite type is analysed.

2 Model

2.1 Interactions between hosts and parasites

The number of parasites affecting a focal host (and vice versa) and the strength of the interactions are key components for models of host-parasite coevolution. Three possible models are depicted in Table 1, where fitness effects are collected in a matrix, which intuitively describes the influence of each type within one species on each type within the other species. Assuming n types of hosts and n types of parasites, M^H describes the average loss of fitness hosts suffer from specific parasite types and M^P describes the average gain of fitness parasites extract from the interaction. For example $(M^H)_{2,4}$ is the fitness loss that host 2 suffers from parasite type 4. On the other hand, $(M^P)_{4,2}$ is what parasite 4 gains from host 2.

To introduce host-parasite dynamics, we focus on the matching allele model first (Grosberg and Hart, 2000; Carius et al., 2001), where only fixed pairs of hosts and parasites can directly interact with each other (Tab. 1, Matching alleles). Interactions with all other partners are neutral and do not influence fitness. In a cross-infection model, it is instead assumed that neighbouring parasite types are genotypically or phenotypically similar in their infectiveness (Tab. 1, Cross-infection). This also applies to each host and its neighbours which have not developed resistance and are therefore susceptible to a specific parasite type which now benefits from three host types. In our model, we assume that cross-infectivity follows periodic boundary conditions where types 1 and n can also interact with three types of the other species. Finally, in our most general model hosts have a positive effect α_i on parasites which have a negative effect $-\alpha_i$ with $c > 0$ on the hosts (Tab. 1, General infection). Every diagonal has a different value, which leads to n interaction parameters. This means that parasite i has the same effect $-\alpha_i$ on host $i + k$ as parasite j on host $j + k$. Further, host i has the same but positive effect α_{i-k} on parasite $i - k$. The restriction $M^H = -c \cdot (M^P)^\top$ ensures a scaled effect of the interaction partners. In this way we can for example envision a scenario in which there are matching hosts and parasites (the main diagonal) and the effect they exert on each other declines with distance between them, $\alpha_1 > \alpha_2 > \alpha_3 > \dots$

Model	M^P	M^H
Matching alleles	$\begin{pmatrix} +1 & 0 & \cdots & 0 \\ 0 & +1 & \cdots & 0 \\ \vdots & \vdots & \ddots & \vdots \\ 0 & 0 & \cdots & +1 \end{pmatrix}$	$\begin{pmatrix} -1 & 0 & \cdots & 0 \\ 0 & -1 & \cdots & 0 \\ \vdots & \vdots & \ddots & \vdots \\ 0 & 0 & \cdots & -1 \end{pmatrix}$
Cross-infection	$\begin{pmatrix} +1 & +1 & 0 & 0 & \cdots & +1 \\ +1 & +1 & +1 & 0 & \cdots & 0 \\ 0 & +1 & +1 & +1 & \cdots & 0 \\ \vdots & \vdots & \vdots & \vdots & \ddots & \vdots \\ 0 & 0 & \cdots & +1 & +1 & +1 \\ +1 & 0 & \cdots & 0 & +1 & +1 \end{pmatrix}$	$\begin{pmatrix} -1 & -1 & 0 & 0 & \cdots & -1 \\ -1 & -1 & -1 & 0 & \cdots & 0 \\ 0 & -1 & -1 & -1 & \cdots & 0 \\ \vdots & \vdots & \vdots & \vdots & \ddots & \vdots \\ 0 & 0 & \cdots & -1 & -1 & -1 \\ -1 & 0 & \cdots & 0 & -1 & -1 \end{pmatrix}$
General infection	$\begin{pmatrix} \alpha_1 & \alpha_2 & \cdots & \alpha_{n-1} & \alpha_n \\ \alpha_n & \alpha_1 & \alpha_2 & \cdots & \alpha_{n-1} \\ \vdots & \alpha_n & \alpha_1 & \cdots & \vdots \\ \alpha_3 & \vdots & \vdots & \ddots & \alpha_2 \\ \alpha_2 & \alpha_3 & \cdots & \alpha_n & \alpha_1 \end{pmatrix}$	$\begin{pmatrix} -c\alpha_1 & -c\alpha_n & \cdots & -c\alpha_3 & -c\alpha_2 \\ -c\alpha_2 & -c\alpha_1 & -c\alpha_n & \cdots & -c\alpha_3 \\ \vdots & -c\alpha_2 & -c\alpha_1 & \cdots & \vdots \\ -c\alpha_{n-1} & \vdots & \vdots & \ddots & -c\alpha_n \\ -c\alpha_n & -c\alpha_{n-1} & \cdots & -c\alpha_2 & -c\alpha_1 \end{pmatrix}$

Table 1: **Interaction models:** M^P is the parasite's (row) gain achieved by a specific host (column). M^H is the host's (row) loss by a parasite (column).

We stress that these matrices are not chosen to represent a particular biological system. Instead, our approach is to consider more complex models beyond the gene for gene or matching allele models and to analyse their dynamics. The fitness effects represented in the matrices now have to be included in our models. We start with a changing population size approach and then turn to constant population size.

2.2 Changing population size

The classical Lotka–Volterra dynamics are usually employed to describe predator-prey systems where the prey reproduces at a constant rate and the predator dies at a constant rate (Lotka, 1925; Volterra, 1928). This allows the population size to change. The predator density is influenced by the abundance of prey and the prey density is influenced by the abundance of predators. The same concept can be applied to host-parasite systems. We assume n different types of hosts and n different types of parasites. The hosts have a constant birth-rate b_h and a death rate that is

determined by the interactions with the parasite. Conversely, we assume a constant parasite death-rate d_p , but a birth rate that depends on the interactions with the hosts. With these assumptions the change of host (h_i) and parasite (p_i) abundance in time can be formulated as

$$\dot{h}_i = h_i (f_i^H + b_h) \quad \text{and} \quad \dot{p}_i = p_i (f_i^P - d_p). \quad (1)$$

The fitness values f_i^H and f_i^P are defined by the interaction matrix and the abundances of the types.

Instead of immediately numerically exploring the dynamics for particular parameter sets, we first aim to obtain some general insight. On the boundaries of the state space, we have one fixed point where hosts and parasites are extinct, $h_i = p_i = 0$ for all i . In the absence of parasites, the host population will continue to increase in size, whereas a parasite population is not viable in the absence of hosts. In terms of co-existence, it is more interesting to consider potential interior fixed points.

For the matching allele model, we have a fixed point where all hosts and parasites have equal abundances, $p_i^* = h_i^* = n^{-1}$ for all i . In this case, the equations completely decouple and each host-parasite pair can evolve independently. Thus, the fixed point is neutrally stable, as for the case of a single host and a single parasite.

For the cross-infection model, a host suffers from three parasite types and each parasite type benefits from three host types. The internal fixed point is now $h_i^* = \frac{d_p}{3}$ and $p_i^* = \frac{b_h}{3}$. For the general model, we obtain $h_i^* = \frac{d_p}{\sum_{i=1}^n \alpha_i}$ and $p_i^* = \frac{b_h}{c \sum_{i=1}^n \alpha_i}$. In both cases, we again find neutral stability (see supplementary material).

In addition, the symmetry of the system leads to a constant of motion. For all three models, the constant of motion is given by (Plank, 1995; Hofbauer and Sigmund, 1998),

$$H = \sum_{i=1}^n h_i - \sum_{i=1}^n h_i^* \log h_i + c \sum_{i=1}^n p_i + c \sum_{i=1}^n p_i^* \log p_i. \quad (2)$$

This implies that the dynamics effectively takes place in a space which has one dimension less.

2.3 Constant population size

As before we assume n different types of hosts and n different types of parasites. The relative abundance of host type i is h_i , the relative abundance of parasite type i is p_i ($i = 1, \dots, n$). With h and p we denote the vectors of the relative abundances. Thus, we have $\sum_{i=1}^n h_i = 1$ as well as $\sum_{i=1}^n p_i = 1$. We assume that the relative abundances change according to the replicator dynamics (Hofbauer and Sigmund, 1998),

$$\dot{h}_i = h_i(t) (f_i^H - \bar{f}^H) \quad \text{and} \quad \dot{p}_i = p_i (f_i^P - \bar{f}^P) \quad (3)$$

where $f_i^H = (M^H p)_i$ is the host fitness for type i and $\bar{f}^H = h M^H p$ is the average fitness of the host population. Similarly, $f_i^P = (M^P h)_i$ is the parasite fitness for type i and $\bar{f}^P = p M^P h$ is the average fitness of the parasite population.

For example, a system with two hosts and two parasites ($n = 2$) where matching hosts and parasites have an influence of $\alpha_1 = 1$ and mismatching pairs exert a smaller fitness effect $\alpha_2 = 0.3$ with a twofold impact on the host $c = 2$ would be a system of four differential equations,

$$\dot{h}_1 = h_1 (-2p_1 - 0.6p_2 - [h_1 (-2p_1 - 0.6p_2) + h_2 (-0.6p_1 - 2p_2)]) \quad (4)$$

$$\dot{h}_2 = h_2 (-0.6p_1 - 2p_2 - [h_1 (-2p_1 - 0.6p_2) + h_2 (-0.6p_1 - 2p_2)]) \quad (5)$$

$$\dot{p}_1 = p_1 (+1h_1 + 0.3h_2 - [p_1 (+1h_1 + 0.3h_2) + p_2 (+0.3h_1 + 1h_2)]) \quad (6)$$

$$\dot{p}_2 = p_2 (+0.3h_1 + 1h_2 - [p_1 (+1h_1 + 0.3h_2) + p_2 (+0.3h_1 + 1h_2)]) \quad (7)$$

Again, this model can now be solved numerically to generate trajectories depending on the initial values of p_1 and h_1 (which determine $p_2 = 1 - p_1$ and $h_2 = 1 - h_1$). However, this approach would only lead to insights about particular parameter sets. Thus, here we take a different and – in our opinion – a more powerful approach and look at general properties of the system.

The replicator dynamics Eq. (3) has fixed points on the edge of the state space, e.g. $h_1 = p_1 = 1$ and $h_i = p_i = 0$ for $i > 1$. However, these fixed points are unstable for a generic parameter choice, which means that a small perturbation from this point drives the system away. There is an

additional fixed point where all types have equal abundance, $p_i^* = h_i^* = n^{-1}$ for all i . This arises from the symmetry of the interaction matrices we consider, but the fixed point can also be verified directly in Eq. (3).

The dynamics of the system depends crucially on the stability of the interior fixed point, which can be attracting, repelling or neutrally stable. For the matching allele model, the interior fixed point is neutrally stable for any number of types (see supplementary material), which implies that a small perturbation from the fixed point does not lead back to it, neither does it increase the distance. In terms of the cross infection models, it is substantially harder to prove this, but in the supplementary material we show that at least for $n \leq 6$, the fixed point remains neutrally stable. Also for the general model, an analysis is intricate. For $n = 3$, we can show that the fixed point remains neutrally stable if the interaction strength decreases with the distance between host and parasite type.

There is a constant of motion, as recognized previously (Hofbauer, 1996)

$$H = \sum_{i=1}^n \log h_i + c \sum_{i=1}^n \log p_i. \quad (8)$$

The existence of such a quantity arises from the symmetry of the system and implies that effectively, the system has one free variable less. However, as we show below, it does not imply any regularity of the dynamics.

2.4 Irregular dynamics in the most simple model

While the general properties discussed above lead to a first insight, e.g. the fact that there is always an interior fixed point and that it is neutrally stable, they do not give insights beyond the fact that the dynamics is oscillatory. Close to the fixed point, one would expect regular oscillations, but it remains unclear what happens if we leave the vicinity of the fixed point.

It turns out that in spite of the constants of motion and neutral stability, the trajectories of host and parasite abundances through time can become irregular and non-periodic. This can already be observed in a three type matching allele model with constant population size, cf. Fig. 1. This surprising result even for the simplest model we consider led us to examine this particular model

more thoroughly.

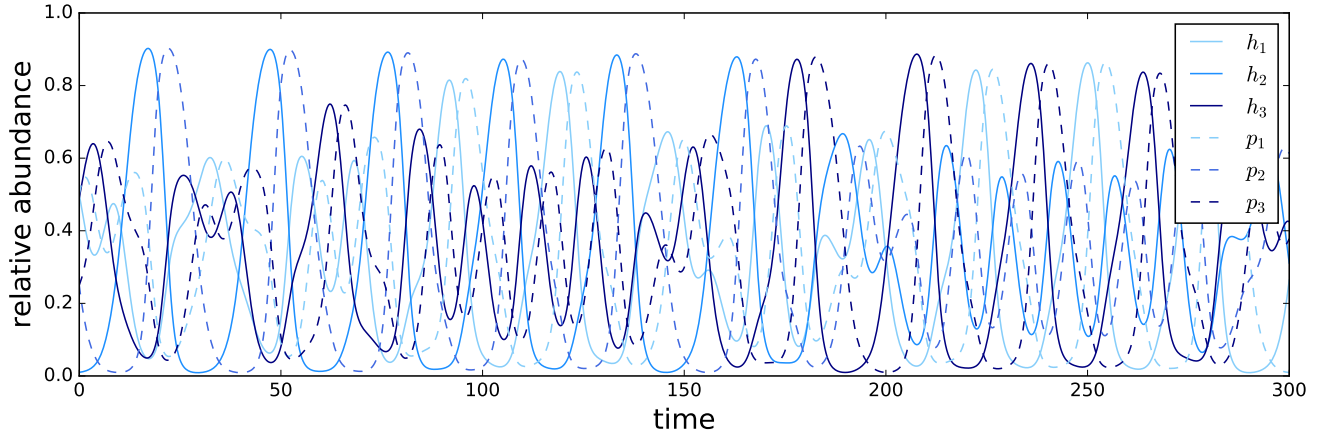


Figure 1: **Matching allele replicator dynamics with three types:** Trajectory of all host and parasite types for a 3-type matching allele replicator dynamics system, Eqs. (3), with initial conditions $h(0) = (0.5, 0.01, 0.49)^\top$ and $p(0) = (0.5, 0.25, 0.25)^\top$. Numerical integration with python’s built-in `odeint` function.

Because of the constant population size, a third type has a relative abundance determined by the abundance of the other two types. For each species the dimensions reduce from three to two. It is therefore possible to show the dynamics for one species in a 3-simplex (Figure 2), where each vertex represents the sole existence of one type, the edges correspond to a coexistence of two types and the interior is a state where no type is extinct. For balanced initial conditions close to the center of the simplex, trajectories are confined to orbits around the interior fixed point. For more extreme initial conditions, starting close to the edge of the simplex, this is no longer true. The trajectory is no longer limited to regular orbits, but nearly fills out the whole simplex, going from conditions close to extinction of one type (edges of simplex) to a near balance of all types (close to the interior fixed point).

To analyse the regularity of the dynamics further, we visualised trajectories of different initial conditions in Poincaré sections to check for chaotic behaviour (Strogatz, 2000). Plotting Poincaré sections is a method to analyse dynamic properties of high dimensional systems. This is implemented by plotting trajectories in a two-dimensional area under certain restrictions (see Fig. 3). Periodic trajectories pass through the section in a periodic way, drawing circles or other closed

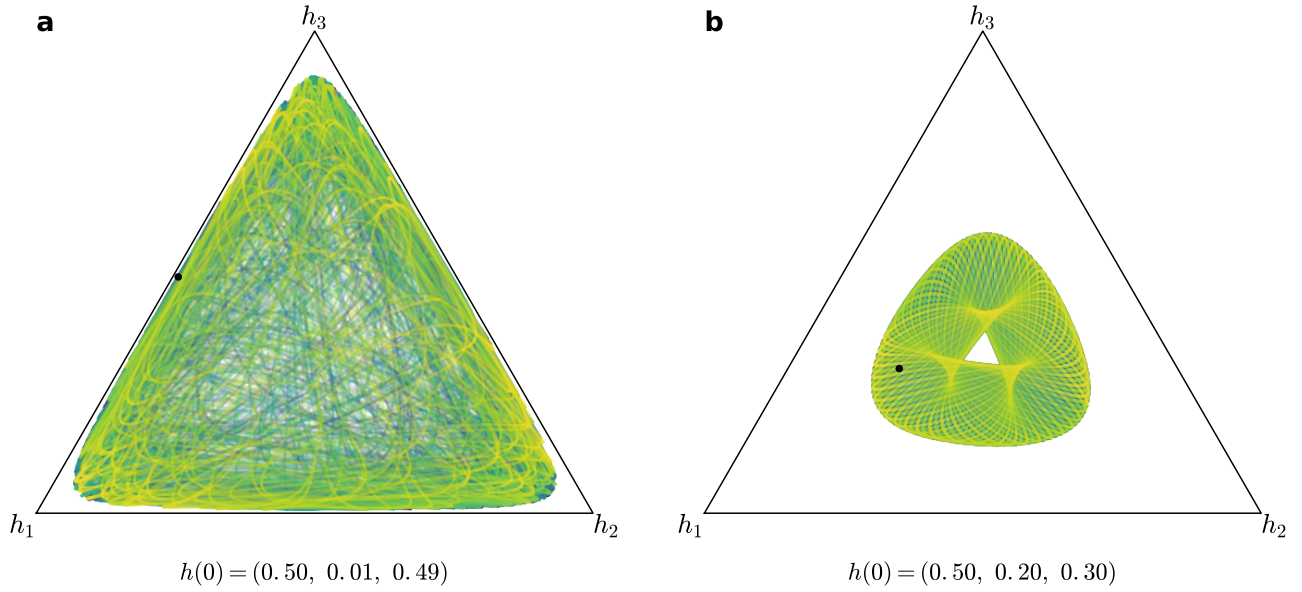


Figure 2: **Matching allele replicator dynamics with three types.** Host 3-simplex for a 3-type matching allele replicator dynamics system with initial conditions given by $h(0)$ and $p(0) = (0.5, 0.25, 0.25)^\top$ indicated as a black dot. Panel (a) corresponds to the initial condition from Fig. 1. Time is represented in the colour gradient going from purple to blue, green and yellow. For initial conditions close to the interior fixed point, the dynamics remains regular (b), but for initial conditions closer to the edges, irregular dynamics emerges (a). Numerical integration was performed using `python`'s built in `odeint` function. Plotted for 10000 (a) and 5000 (b) generations.

trajectories. Chaotic trajectories have a much less ordered path and thus scatter over a larger part of the section. In [Sato et al. \(2002\)](#) chaotic behaviour and large positive Lyapunov exponents were found for several initial conditions in a two-person rock-paper-scissors learning game. This is formally closely related to a replicator dynamics host-parasite system with three types. We utilised this approach for our matching allele model and numerically evaluated several initial conditions. As expected from the neutrally stable fixed points, closed and periodic trajectories are found in [Figure 3](#) for most initial conditions. For initial conditions close to the edge of the state space, the trajectories become visibly scattered.

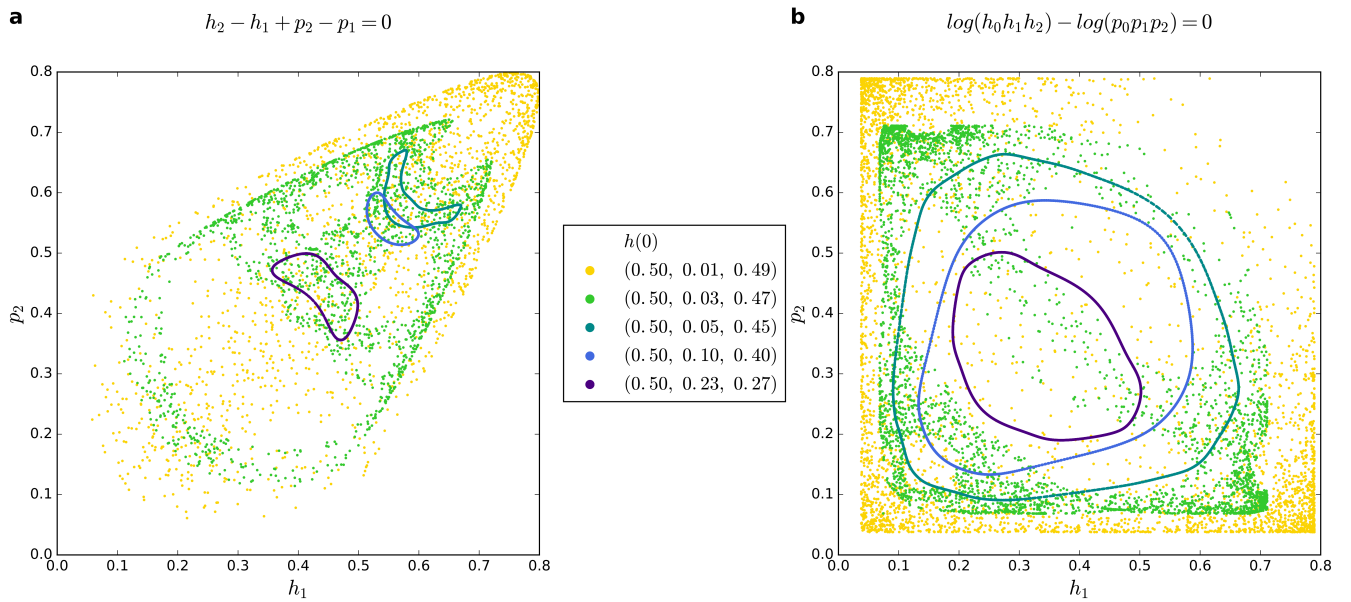


Figure 3: Poincaré sections for a 3-type matching allele replicator dynamics system: The Poincaré sections with restrictions $|h_2 - h_1 + p_2 - p_1| \leq 0.001$ ((a), following [Sato et al. \(2002\)](#)) and $|\log h_1 h_2 h_3 - \log p_1 p_2 p_3| \leq 0.001$ (b) are plotted. The horizontal and vertical axes are the host type 1, h_1 and parasite type 2, p_2 respectively. Initial conditions for $h(0)$ are as stated in the legend and $p(0) = (0.5, 0.25, 0.25)^\top$. For initial conditions closer to the fixed point (dark green, blue, purple, see also [Fig. 2 b](#)), the trajectories show periodic behaviour in a higher dimension. For extreme initial conditions, close to the edge of the state space (yellow, light green, see also [Fig. 2 a](#)), the trajectories become chaotic and show a wide spread over the state space. Numerical integration was performed using `python`'s built in `odeint` function, for 50000 generations.

3 Discussion

[Stenseth and Maynard Smith \(1984\)](#) as well as [Nordbotten and Stenseth \(2016\)](#) showed that

only trophic $+/-$ interactions (as opposed to mutualism $+/+$ or competition $-/-$) promote Red Queen dynamics independent of abiotic factors. This justifies our study of these dynamics in a simple framework without abiotic influence or other types of interactions than trophic. Red Queen dynamics have been repeatedly reported to occur in models with two types, often because two alleles were in focus in the matching allele or gene-for-gene model (Schmid-Hempel and Jokela, 2002; Frank, 1993b; Flor, 1956; Agrawal and Lively, 2002; Song et al., 2015). A clear focus on multiple types has, to our knowledge, not been extensively analysed before. Yet, examples from observed biological systems clearly motivate the need for including this aspect into theoretical studies (Carius et al., 2001; Koskella and Lively, 2009; Luijckx et al., 2014). Rabajante et al. (2015) numerically investigated such host-parasite systems with multiple types. We study host-parasite coevolution with three successively complicated interaction matrices in frameworks with more than two types where both constant and changing population size models can be justified (MacArthur, 1970).

We allow for n different interaction parameters in the most general payoff matrix. It is an advantage to be able to calculate specific outcomes with analytically derived statements and not have to rely entirely on numerical integration with fixed parameters and fixed initial conditions. For the same reason, we focus on a deterministic framework, allowing broad predictions. Eventually, one also has to include stochastic effects, which can have decisive impact on coevolutionary dynamics, in particular when the dynamics reaches the edges of the state space where extinction is likely (Gokhale et al., 2013). Also to explore signatures of genomic selection, such as selective sweeps or balancing selection, this is necessary (Tellier et al., 2014).

The presence of neutrally stable fixed points and constants of motion may lead to the belief that Red Queen dynamics exist on stable, regular orbits around the interior fixed point. These are also often shown to illustrate this kind of dynamics. The fixed points are neither repelling, thereby forbidding a coexistence of this type, nor attracting and, therefore, leading to a stable equilibrium. A neutrally stable fixed point and the consequent concentric circles, spheres or higher dimensional circulations around the point mean that the system is constantly changing, and yet, stationary in this change. Formulating constants of motions or Hamiltonians underlines this principle. However,

the stability of a fixed point only holds locally and a constant of motion is a purely mathematical constraint. In general, the neutral stability supports the notion of Red Queen cycling. To understand this kind of dynamics in more detail, we have focused on the simplest possible dynamics and not attempted to construct a model for a concrete biological scenario. It is possible to consider more complex dynamics with stable or unstable interior fixed points or even limit cycles. However, our goal is to illustrate that even these simple models, which often form the basis for investigations of host parasite coevolution, can show a dynamics which is much richer than one would expect from verbal arguments or numerical considerations of such systems close to interior fixed points.

Simple models built on differential equations have been famously known to show chaotic properties in the sense that close by starting conditions can lead to very diverse outcome, thus restricting the predictability of the dynamics to very short time horizons (Lorenz, 1963; May, 1976; Hamilton et al., 1990; Hassell et al., 1991; Schuster, 1995; Sato et al., 2002). It thus comes as no surprise that a system of multiple interacting species can lead to chaos in some parts of the parameter space (May and Leonard, 1975; Smale, 1976). Recently Duarte et al. (2015) found chaos in a food chain model with three species resulting in Red Queen dynamics. There is general interest in increasing the number of species in the analysis (Liow et al., 2011; Dercole et al., 2010). However, to our knowledge, chaos has never been linked to Red Queen dynamics in a two-species model.

For multiple (three and more) types, we found that trajectories starting further away from the interior fixed point can show such chaotic behaviour. Chaotic fluctuations of host and parasite abundances, therefore, become possible in parts of the parameter space. A new type can be introduced to a system exhibiting typical Red Queen oscillations, e.g. via mutation or migration. While the mutant appears at low frequencies, the system shifts to an edge in a higher dimension. Our analysis predicts that this might often lead to chaotic dynamics rather than to stasis or the persistence of regular Red Queen oscillations. The typical, Red Queen dynamics is thought to consist of regular sinusoid-like oscillations of the frequencies of the different types within host and parasite populations with short periods and one or few amplitudes. We are now facing highly irregular trajectories without periodic re-occurrence and different magnitudes of maxima in each cycle. With our model, we propose that in addition to the concepts of stasis or regular Red Queen

cycling a third scenario - chaotic Red Queen dynamics - is possible and likely. Chaos, then, would be especially rampant in the presence of low levels of standing genetic variation, mutations and migration. Moreover, it would in particular occur for very large populations, where the typical intuition of evolutionary biologists is to expect regular deterministic dynamics.

Acknowledgments

We thank Hinrich Schulenburg for fruitful discussions and comments on the manuscript. Generous funding by the Max Planck Society is gratefully acknowledged. CSG acknowledges funding from the New Zealand Institute for Advanced Study and support from the Marsden Fund Council administered by the Royal Society of New Zealand. The authors declare no conflict of interests.

References

- Agrawal, A. and C. M. Lively, 2002. Infection genetics: gene-for-gene versus matching-alleles models and all points in between. *Evolutionary Ecology Research* 4:79–90.
- Brockhurst, M. A., T. Chapman, K. C. King, J. E. Mank, S. Paterson, and G. D. D. Hurst, 2014. Running with the Red Queen: the role of biotic conflicts in evolution. *Proceedings of the Royal Society B: Biological Sciences* 281:20141382–20141382.
- Carius, H. J., T. J. Little, and D. Ebert, 2001. Genetic variation in a host-parasite association: potential for coevolution and frequency-dependent selection. *Evolution* 55:1136–1145.
- Clay, K. and P. X. Kover, 1996. The red queen hypothesis and plant/pathogen interactions. *Annual Review of Phytopathology* 34:29–50.
- Decaestecker, E., S. Gaba, J. A. M. Raeymaekers, L. v. K. R. Stoks, D. Ebert, and L. D. Meester, 2007. Host–parasite ‘red queen’ dynamics archived in pond sediment. *Nature* 450:870–873.
- Dercole, F., R. Ferriere, and S. Rinaldi, 2010. Chaotic red queen coevolution in three-species food chains. *Proceedings of the Royal Society B* 277:2321–2330.

- Dieckmann, U., P. Marrow, and R. Law, 1995. Evolutionary cycling in predator–prey interactions: Population dynamics and the red queen. *Journal of Theoretical Biology* 176:91–102.
- Duarte, J., C. Rodrigues, C. Januário, N. Martins, and J. Sardanyés, 2015. How complex, probable, and predictable is genetically driven red queen chaos? *Acta Biotheoretica* 63:341–361.
- Engelstädter, J., 2015. Host-parasite coevolutionary dynamics with generalized success/failure infection genetics. *The American Naturalist* .
- Flor, H. H., 1955. Host-parasite interaction in flax rust - its genetics and other implications. *Phytopathology* 45:680–685.
- , 1956. The complementary genetic systems in flax and flax rust. *Advances in Genetics* 8:29–54.
- Frank, S. A., 1993a. Coevolutionary genetics of plants and pathogens. *Evolutionary Ecology* 7:45–75.
- , 1993b. Specificity versus detectable polymorphism in host–parasite genetics. *Proceedings of the Royal Society of London. Series B: Biological Sciences* 254:191–197.
- , 1996. Problems inferring the specificity of plant—pathogen genetics. *Evolutionary Ecology* 10:323–325.
- Gokhale, C. S., A. Papkou, A. Traulsen, and H. Schulenburg, 2013. Lotka-Volterra dynamics kills the Red Queen: population size fluctuations and associated stochasticity dramatically change host-parasite coevolution. *BMC Evolutionary Biology* 13:254.
- Grosberg, R. K. and M. W. Hart, 2000. Mate selection and the evolution of highly polymorphic self/nonspecific recognition genes. *Science* 289:2111–2114.
- Hamilton, W. D., R. Axelrod, and R. Tanese, 1990. Sexual reproduction as an adaptation to resist parasites (a review). *Proceedings of the National Academy of Sciences* .
- Hassell, M. P., H. N. Comins, and R. M. May, 1991. Spatial structure and chaos in insect population dynamics. *Nature* 353:255–258.

- Hofbauer, J., 1996. Evolutionary dynamics for bimatrix games: A Hamiltonian system? *Journal of Mathematical Biology* 34:675–688.
- Hofbauer, J. and K. Sigmund, 1998. *Evolutionary Games and Population Dynamics*. Cambridge University Press, Cambridge, UK.
- Koskella, B. and C. M. Lively, 2009. Evidence for negative frequency-dependent selection during experimental coevolution of a freshwater snail and sterilizing trematode. *Evolution* 63:2213–2221.
- Liow, L. H., L. Van Valen, and N. C. Stenseth, 2011. Red queen: from populations to taxa and communities. *Trends in Ecology & Evolution* 26:349–358.
- Lively, C. M., 2010. A review of red queen models for the persistence of obligate sexual reproduction. *Journal of Heredity* 101:S13–S20.
- Lorenz, E. N., 1963. Deterministic non-periodic flow. *Journal of the Atmospheric Sciences* 20:130–141.
- Lotka, A. J., 1925. *Elements of Physical Biology*. Baltimore.
- Luijckx, P., D. Duneau, J. P. Andras, and D. Ebert, 2014. Cross-species infection trials reveal cryptic parasite varieties and a putative polymorphism shared among host species. *Evolution* 68:577–586.
- MacArthur, R., 1970. Species packing and competitive equilibrium for many species. *Theoretical Population Biology* Pp. 1–11.
- May, R. M., 1976. Simple mathematical models with very complicated dynamics. *Nature* 261:459–467.
- May, R. M. and W. J. Leonard, 1975. Nonlinear aspects of competition between three species. *SIAM Journal on Applied Mathematics* 29:243–253.
- Maynard Smith, J., 1976. A Comment on the Red Queen. *American Naturalist* 110:325–330.

- Metzger, C. M. J. A., P. Luijckx, G. Bento, M. Mariadassou, and D. Ebert, 2016. The Red Queen lives: Epistasis between linked resistance loci. *Evolution* 70:480–487.
- Nordbotten, J. M. and N. C. Stenseth, 2016. Asymmetric ecological conditions favor red-queen type of continued evolution over stasis. *Proceedings of the National Academy of Sciences USA* .
- Papkou, A., C. S. Gokhale, A. Traulsen, and H. Schulenburg, 2016. Host parasite coevolution: Why changing population size matters? *Zoology* in press.
- Parker, M. A., 1996. The nature of plant—parasite specificity. *Evolutionary Ecology* 10:319–322.
- Plank, M., 1995. Hamiltonian structures for the n -dimensional lotka-volterra equations. *Journal of Mathematical Physics* 36:3520–3534.
- Rabajante, J. F., J. M. Tubay, T. Uehara, S. Morita, D. Ebert, and J. Yoshimura, 2015. Red queen dynamics in multi-host and multi-parasite interaction systems. *Scientific Reports* .
- Salathé, M., R. Kouyos, and S. Bonhoeffer, 2008. The state of affairs in the kingdom of the Red Queen. *Trends in Ecology & Evolution* 23:439–445.
- Sasaki, A., 2000. Host-parasite coevolution in a multilocus gene-for-gene system. *Proceedings of the Royal Society B: Biological Sciences* 267:2183–2188.
- Sato, Y., E. Akiyama, and J. D. Farmer, 2002. Chaos in learning a simple two-person game. *Proceedings of the National Academy of Sciences USA* 99:4748–4751.
- Schmid-Hempel, P. and J. Jokela, 2002. Socially structured populations and evolution of recombination under antagonistic coevolution. *The American Naturalist* 160:403–408.
- Schuster, H. G., 1995. *Deterministic Chaos*. 3rd ed. VCH, Weinheim.
- Schuster, P. and K. Sigmund, 1983. Replicator dynamics. *Journal of Theoretical Biology* 100:533–538.
- Smale, S., 1976. On the differential equations of species in competition. *Journal of Mathematical Biology* 3:5–7.

- Song, Y., C. S. Gokhale, A. Papkou, H. Schulenburg, and A. Traulsen, 2015. Host-parasite coevolution in populations of constant and variable size. *BMC Evolutionary Biology* 15:212.
- Stenseth, N. C. and J. Maynard Smith, 1984. Coevolution in ecosystems: Red queen evolution or stasis? *Evolution* 38:870–880.
- Strogatz, S., 2000. *Nonlinear Dynamics and Chaos: With Applications to Physics, Biology, Chemistry, and Engineering (Studies in Nonlinearity)*. Westview Pr.
- Taylor, P. D. and L. Jonker, 1978. Evolutionarily stable strategies and game dynamics. *Mathematical Biosciences* 40:145–156.
- Tellier, A., S. Moreno-Gómez, and W. Stephan, 2014. Speed of adaptation and genomic footprints of host-parasite coevolution under arms race and trench warfare dynamics. *Evolution* 68:2211–2224.
- van Valen, L., 1973. A new evolutionary law. *Evolutionary Theory* 1:1–30.
- Van Valen, L., 1977. The Red Queen. *The American Naturalist* 111:809–810.
- Volterra, V., 1928. Variations and fluctuations of the number of individuals in animal species living together. *Journal du conseil international pour l’exploration de la mer* 3:3–51.

Supplementary material

1 Models

1.1 Replicator dynamics

The specific models, defined by the matrices in Table 1 in the main text are now applied to replicator dynamics. This leads to a differential equation for each h_i and p_i , where $i = 1, \dots, n$.

Matching allele: Even though this model is based on interaction between matching types, owing to the constant population size there is an indirect effect of other hosts and parasites on one another. Biologically, this can e.g. reflect competition between hosts. For example, if one host increases fast in numbers or when space, food or other resources are limited other hosts suffer from the increase of that specific type and decrease in abundance. Applying the matching allele fitness effects to replicator dynamics leads to a set of coupled differential equations which describe the frequency change of host and parasite types,

$$\dot{h}_i = h_i \left(-p_i + \sum_{k=1}^n h_k p_k \right) \qquad \dot{p}_i = p_i \left(h_i - \sum_{k=1}^n h_k p_k \right). \quad (\text{S1})$$

Cross-infection: Because of the periodic boundary condition with $p_0 = p_n$, $p_{n+1} = p_1$, $h_0 = h_n$

and $h_{n+1} = h_1$, it is possible to simplify the differential equations,

$$\dot{h}_i = h_i \left(- (p_{i-1} + p_i + p_{i+1}) + \sum_{k=1}^n h_k (p_{k-1} + p_k + p_{k+1}) \right) \quad (\text{S2})$$

$$\dot{p}_i = p_i \left((h_{i-1} + h_i + h_{i+1}) - \sum_{k=1}^n p_k (h_{k-1} + h_k + h_{k+1}) \right). \quad (\text{S3})$$

General infection: The differential equations are now more complicated, so that it is best to present the general form,

$$\dot{h}_i = h_i \left((M^H p)_i - h^T M^H p \right) \quad \dot{p}_i = p_i \left((M^P h)_i - p^T M^P h \right). \quad (\text{S4})$$

1.2 Lotka–Volterra dynamics

Next, we combine the interaction models from Table 1 with the Lotka–Volterra dynamics.

Matching allele: Again, we first focus on the matching allele model. Since b_h and d_p are constants, the differential equations are decoupled. We thus obtain n independent systems of two differential equations each,

$$\dot{h}_i = h_i (-p_i + b_h) \quad \dot{p}_i = p_i (h_i - d_p), \quad (\text{S5})$$

where $i = 1, \dots, n$. This makes the Lotka–Volterra matching allele model a limiting case, with particularly simple dynamics.

Cross-infection: The differential equations are now connected to each other by types $i \pm 1$,

$$\dot{h}_i = h_i \left(- (p_{i-1} + p_i + p_{i+1}) + b_h \right) \quad \dot{p}_i = p_i \left((h_{i-1} + h_i + h_{i+1}) - d_p \right) \quad (\text{S6})$$

with $p_0 = p_n$, $p_{n+1} = p_1$, $h_0 = h_n$ and $h_{n+1} = h_1$.

General infection: Utilising the most general payoff matrices leads to these general differen-

tial equations

$$\dot{h}_i = h_i \left((M^H p)_i + b_h \right) \quad \text{and} \quad \dot{p}_i = p_i \left((M^P h)_i - d_p \right), \quad (\text{S7})$$

where p and h are the vectors containing all population sizes h_i and p_i for $i = 1, 2, \dots, n$.

2 Stability

A stability analysis of fixed points is conducted by calculating the eigenvalues of the Jacobian matrix at the interior fixed point. The real part of the eigenvalues of this matrix gives insight into the stability of the point. If all are negative the fixed point is attractive, if at least one is positive it is a saddle (and repelling if all are positive) and if all are zero it is neutrally stable. These statements hold locally, which means close to the point of interest, since this is where the Jacobian is evaluated. In the case of replicator dynamics it is possible to reduce the number of differential equations to $2(n-1)$ because of the normalisation $\sum_{i=1}^n h_i = \sum_{i=1}^n p_i = 1$. The matrix now has full rank and the number of eigenvalues is always $2(n-1)$. The Jacobian is further explained in Sec. 2. For deriving fixed points and stability for fixed n , `Mathematica` (?) was used. Solving the differential equations $\dot{h}_i(h^*, p^*) = 0$ and $\dot{p}_i(h^*, p^*) = 0$ leads to some trivial fixed points where at least one host or one parasite type are extinct.

Jacobian matrix

In general the Jacobian for replicator dynamics is

$$J = \begin{pmatrix} \frac{\partial \dot{h}_1}{\partial h_1} & \dots & \frac{\partial \dot{h}_1}{\partial h_{n-1}} & \frac{\partial \dot{h}_1}{\partial p_1} & \dots & \frac{\partial \dot{h}_1}{\partial p_{n-1}} \\ \vdots & & \vdots & \vdots & & \vdots \\ \frac{\partial \dot{h}_{n-1}}{\partial h_1} & \dots & \frac{\partial \dot{h}_{n-1}}{\partial h_{n-1}} & \frac{\partial \dot{h}_{n-1}}{\partial p_1} & \dots & \frac{\partial \dot{h}_{n-1}}{\partial p_{n-1}} \\ \hline \frac{\partial \dot{p}_1}{\partial h_1} & \dots & \frac{\partial \dot{p}_1}{\partial h_{n-1}} & \frac{\partial \dot{p}_1}{\partial p_1} & \dots & \frac{\partial \dot{p}_1}{\partial p_{n-1}} \\ \vdots & & \vdots & \vdots & & \vdots \\ \frac{\partial \dot{p}_{n-1}}{\partial h_1} & \dots & \frac{\partial \dot{p}_{n-1}}{\partial h_{n-1}} & \frac{\partial \dot{p}_{n-1}}{\partial p_1} & \dots & \frac{\partial \dot{p}_{n-1}}{\partial p_{n-1}} \end{pmatrix} \in \mathbb{R}^{2(n-1) \times 2(n-1)} \quad (\text{S8})$$

and similar in the Lotka–Volterra case but in $\mathbb{R}^{2n \times 2n}$, where the number of eigenvalues is $2n$.

Replicator dynamics: Matching allele model

After reducing dimensions with $h_n = 1 - \sum_{i=1}^{n-1} h_i$ and $p_n = 1 - \sum_{i=1}^{n-1} p_i$ the differential equations are defined for $i = 1, 2, \dots, n-1$:

$$\dot{h}_i = h_i \left(-p_i + \sum_{k=1}^{n-1} h_k p_k + \left(1 - \sum_{k=1}^{n-1} h_k \right) \left(1 - \sum_{k=1}^{n-1} p_k \right) \right) \quad (\text{S9})$$

and

$$\dot{p}_i = p_i \left(h_i - \sum_{k=1}^{n-1} h_k p_k - \left(1 - \sum_{k=1}^{n-1} h_k \right) \left(1 - \sum_{k=1}^{n-1} p_k \right) \right) \quad (\text{S10})$$

The Jacobian at the interior fixed point $h_i^* = p_i^* = \frac{1}{n}$ simplifies to

$$J(h^*, p^*) = \begin{pmatrix} 0 & -\frac{1}{n} & 0 \\ & \ddots & \\ \frac{1}{n} & 0 & -\frac{1}{n} \\ & \ddots & \\ 0 & \frac{1}{n} & 0 \end{pmatrix} \in \mathbb{R}^{2(n-1) \times 2(n-1)}. \quad (\text{S11})$$

The eigenvalues of the Jacobian matrix are calculated via the determinant $\det(J(h^*, p^*) - \lambda I_{2(n-1)})$ which is not changed by adding multiples $(\frac{1}{\lambda n})$ of the upper $n-1$ rows to the lower $n-1$. This leads to the following matrix

$$\begin{pmatrix} -\lambda & -\frac{1}{n} & 0 \\ & \ddots & \\ -\lambda & 0 & -\frac{1}{n} \\ 0 & -\lambda - \frac{1}{\lambda n^2} & 0 \\ & \ddots & \\ 0 & 0 & -\lambda - \frac{1}{\lambda n^2} \end{pmatrix}. \quad (\text{S12})$$

The determinant of this matrix is the product of the diagonal elements. The following equation determines the eigenvalues:

$$\begin{aligned} 0 &= (-\lambda)^{n-1} \left(-\lambda - \frac{1}{\lambda n^2} \right)^{n-1} \\ &= \left(\lambda + i\frac{1}{n} \right)^{n-1} \left(\lambda - i\frac{1}{n} \right)^{n-1} \end{aligned} \quad (\text{S13})$$

The eigenvalues are $\lambda = \pm i\frac{1}{n}$ with multiplicity $n-1$. This means that the interior fixed point is neutrally stable and the oscillation frequency close to this point is $\frac{1}{2\pi n}$. This implies that the period of the oscillation $2\pi n$ depends on the number of types of host and parasite. The oscillation

with n types has an oscillation period which is n times slower than in a system with only one host and parasite type. In the case of replicator dynamics, this is based on the coupling through the average fitness \bar{f} .

Replicator dynamics: cross-infection

In the more complicated cross-infection model it is challenging to solve the problem for general n which is why a stability analysis is shown for several fixed n . For $n = 4$, we find

$$\lambda = \pm \frac{i}{4} \quad \text{each with multiplicity 3.} \quad (\text{S14})$$

For $n = 5$, we find

$$\lambda = \pm \frac{i}{5} \sqrt{\frac{1}{2} (3 \pm \sqrt{5})} \quad \text{each with multiplicity 2.}$$

For $n = 6$, we have

$$\begin{aligned} \lambda_1 &= 0 && \text{with multiplicity 4,} \\ \lambda_2 &= \pm \frac{i}{3} && \text{each with multiplicity 2,} \\ \lambda_3 &= \pm \frac{i}{6} && \text{each with multiplicity 1.} \end{aligned} \quad (\text{S15})$$

The fixed point is neutrally stable in all cases.

Replicator dynamics: general model

In this general case the stability is analysed in the case of $n = 3$. The four eigenvalues depend on the payoffs:

$$\lambda = \pm \frac{\sqrt{c}}{3} \sqrt{\pm (\alpha_2^H - \alpha_3^H) - (\alpha_1^H - \alpha_2^H) (\alpha_1^H - \alpha_3^H)} \quad (\text{S16})$$

The interior fixed point is neutrally stable if all eigenvalues are zero or without exception imaginary. This holds if the term under the square root is negative in all cases. This is the case if the second term is larger than the first, which implies $\alpha_1^H \gg \alpha_2^H > \alpha_3^H$. Thus, assuming that more distant hosts are less suitable for the parasite, the fixed point is neutrally stable. If however there are two significant host types for each parasite and only one host is unsuitable $\alpha_1^H > \alpha_2^H \gg \alpha_3^H$ then two eigenvalues are real. In that case, we would have a saddle. In other cases it depends on the value of the real part of the eigenvalues. When all eigenvalues are positive the fixed point is not stable (repelling) if all are negative then the fixed point is stable (attractive).

Lotka–Volterra: cross-infection

For $n = 4$, the eigenvalues are

$$\begin{aligned}\lambda_1 &= \pm \frac{i}{3} \sqrt{b_h d_p} && \text{each with multiplicity 3,} \\ \lambda_2 &= \pm i \sqrt{b_h d_p} && \text{each with multiplicity 1.}\end{aligned}\tag{S17}$$

For $n = 5$, the eigenvalues are

$$\begin{aligned}\lambda_1 &= \pm \frac{i}{3\sqrt{2}} \sqrt{(3 \pm \sqrt{5}) b_h d_p} && \text{each with multiplicity 2,} \\ \lambda_2 &= \pm i \sqrt{b_h d_p} && \text{each with multiplicity 1.}\end{aligned}\tag{S18}$$

For $n = 6$, the eigenvalues are

$$\begin{aligned}\lambda_1 &= 0 && \text{with multiplicity 4,} \\ \lambda_2 &= \pm \frac{i}{3} \sqrt{b_h d_p} && \text{each with multiplicity 1,} \\ \lambda_3 &= \pm \frac{2i}{3} \sqrt{b_h d_p} && \text{each with multiplicity 2,} \\ \lambda_4 &= \pm i \sqrt{b_h d_p} && \text{each with multiplicity 1.}\end{aligned}\tag{S19}$$

In all cases analysed the interior fixed point is neutrally stable.

Lotka–Volterra: general model

The eigenvalues for $n = 3$ are

$$\lambda_1 = \pm i\sqrt{b_h d_p} \quad \text{each with multiplicity 1,} \quad (\text{S20})$$

$$\lambda_2 = \pm i\sqrt{b_h d_p} \frac{\sqrt{\alpha_1^H (\alpha_1^H - \alpha_2^H) + \alpha_2^H (\alpha_2^H - \alpha_3^H) - \alpha_3^H (\alpha_1^H - \alpha_3^H)}}{\alpha_1^H + \alpha_2^H + \alpha_3^H} \quad (\text{S21})$$

each with multiplicity 2.

Assuming that interactions with more distant hosts become weaker, $\alpha_1^H > \alpha_2^H > \alpha_3^H$, the term under the square root becomes positive and all eigenvalues have a real part zero. This implies neutral stability of the interior fixed point for $n = 3$.

3 Python code

3.1 Figure 1

```
# -*- coding: utf-8 -*-
"""
@author: schenk
Plot Trajectory for a host-parasite system using Replicator Dynamics
assuming Matching Allele interactions (see a,b,e)
in 3 types of host and 3 types of parasites (n=3)
"""
from scipy.integrate import odeint
import matplotlib.pyplot as plt
import numpy as np
plt.close("all") # close figures
=====
# Variables and settings
=====
a=-1. #alpha1
b=0. #alpha2
e=0. #alpha3
mh=np.array([[a,b,e],[e,a,b],[b,e,a]]) #payoff matrix for host
c=1. #factor for payoff matrix
k=1 #for initial condition
h0=np.array([0.5,0.01*k,0.5-0.01*k]) #initial host frequency
p0=np.array([0.5,0.25,0.25]) #initial parasite frequency
generations=300. #time
```

```

steps=1001. #steps to plot
n=len(h0) #number of types n
mp=-c*mh #payoff matrix for parasite
=====
# Solving of ODE
=====
def deriv(y,t):
    h=y[:n]
    p=y[n:]
    h=h/sum(h) #normalisation
    p=p/sum(p) #normalisation
    dH=np.dot(mh,p) #host fitness defined by interaction with parasite
    bh=np.dot(dH,h) #average host fitness
    hdot=h*(dH-bh) #ODE for host frequency change
    bP=np.dot(mp,h) #parasite fitness defined by interaction with host
    dp=np.dot(bP,p) #average parasite fitness
    pdot=p*(bP-dp) #ODE for parasite frequency change
    return np.concatenate([hdot,pdot])
time = np.linspace(0.0,generations,steps) # start,end,steps
y = odeint(deriv,np.concatenate([h0,p0]),time)
h=y[:n,:] #host frequencies for all time steps
p=y[n:,:] #parasite frequencies for all time steps
=====
# Plot relative abundance (frequencies), time dependent
=====
fig,axes=plt.subplots(nrows=1,ncols=1,figsize=(12,5))
h1, =axes.plot(time,h[:,0],color="lightskyblue",label=r'$h_1$')
h2, =axes.plot(time,h[:,1],color="dodgerblue",label=r'$h_2$')
h3, =axes.plot(time,h[:,2],color="navy",label=r'$h_3$')
p1, =axes.plot(time,p[:,0],color="lightskyblue",linestyle='--',
label=r'$p_1$')
p2, =axes.plot(time,p[:,1],color="royalblue",linestyle='--',
label=r'$p_2$')
p3, =axes.plot(time,p[:,2],color="navy",linestyle='--',
label=r'$p_3$')
axes.set_ylim([0,1])
axes.legend()
axes.set_ylabel('relative abundance',fontsize=18)
axes.set_xlabel('time',fontsize=18)
axes.set_aspect(90)
fig.subplots_adjust(top=1,bottom=0,left=0.07,right=0.98)
fig.savefig("trajectory.pdf")
plt.show()

```

3.2 Figure 2

```

# -*- coding: utf-8 -*-
"""
@author: schenk

```

```

Plot 3-simplex for replicator dynamics with two species
(host, parasite).
Three types each. Matching allele model (a=-1, b=e=0)
"""
from scipy.integrate import odeint
import matplotlib.pyplot as plt
import numpy as np
import math

plt.close("all") # close figures

#=====
# Variables and settings
#=====
a=-1.
b=0.
e=0.
mh=np.array([[a,b,e],[e,a,b],[b,e,a]]) #payoff matrix for host
c=1. #factor
k=1. #initial condition (1 or 10)
cm = plt.cm.get_cmap('viridis')
#figure for host simplex:
fig, axes = plt.subplots(nrows=1,ncols=2,figsize=(12,6))

#for two initial conditions different number of generations:
for k in [1,20]:
    if k==1:
        generations=10000
        steps=1000000.
    else:
        generations=5000
        steps=500000.
    time = np.linspace(0.0,generations,steps) # start,end,steps
    h0=np.array([0.5,0.01*k,0.5-0.01*k]) #initial host frequencies
    p0=np.array([0.5,0.25,0.25]) #initial parasite frequencies

    n=len(h0) #number of hosts or parasites
    mp=-c*mh #payoff matrix for parasites

#=====
# Solving of ODE
#=====

def deriv(y,t):
    h=y[:n] #host frequencies
    p=y[n:] #parasite frequencies
    h=h/sum(h) #normalisation
    p=p/sum(p) #normalisation
    dH=np.dot(mh,p) #host fitness influenced by parasites

```

```

bh=np.dot(dH,h) #average host fitness
hdot=h*(dH-bh) #ODE for hosts
bP=np.dot(mp,h) #parasite fitness influenced by host
dp=np.dot(bP,p) #average parasite fitness
pdot=p*(bP-dp) #ODE for parasites
return np.concatenate([hdot,pdot]) #all ODEs

#numerical integration
y = odeint(deriv,np.concatenate([h0,p0]),time)
h=y[:,n:] #host frequencies
p=y[:,n:] #parasite frequencies

#=====
# Plot Simplex
#=====

# Projection:
proj=np.array([[-math.cos(30./360.*2.*math.pi),
math.cos(30./360.*2.*math.pi),0.],
[-math.sin(30./360.*2.*math.pi),
-math.sin(30./360.*2.*math.pi),1.]])

#2D plot values for host frequencies:
[hx,hy] = np.array(np.mat(proj)*np.mat(h.T))
#2D plot values for parasite frequencies:
[px,py] = np.array(np.mat(proj)*np.mat(p.T))
if k==1:
ax=axes[0]
else:
ax=axes[1]
timeplot=ax.scatter(hx,hy,marker=".",alpha=0.05,c=time, cmap=cm,
edgecolors="none",rasterized=True) #host plot

ax.scatter(hx[0],hy[0],marker='.',s=100,color="black",
edgecolors="none") #initial condition host

trianglepoints=np.hstack([np.identity(3),
np.array([[1.],[0.],[0.]])]) #vertices
triangleline=np.array(np.mat(proj)*np.mat(trianglepoints)) #edges
ax.plot(triangleline[0],triangleline[1],clip_on=False,
color="black",zorder=1) #plot edges for host simplex

# plot options:
ax.annotate("$h_1$",xy=(0,0),xycoords="axes fraction",
ha="right",va="top",fontsize=18,color="black")
ax.annotate("$h_2$",xy=(1,0),xycoords="axes fraction",
ha="left",va="top",fontsize=18,color="black")
ax.annotate("$h_3$",xy=(0.5,1),xycoords="axes fraction",
ha="center",va="bottom",fontsize=18,color="black")
ax.annotate("$h(0)=(\$"+ "${:,.2f}$".format(h0[0])+'$, $ '+

```

```

"${:,.2f}$".format(h0[1])+'$, $ '+
"${:,.2f}$".format(h0[2])+'$)$',
xy=(0.5,-0.1),xycoords="axes fraction", ha="center",
va="top",fontSize=16)
ax.set_xlim([triangleline[0,0],triangleline[0,1]]) #limit x-axis
ax.set_ylim([-0.5,1.]) #limit y-axis
ax.set_xlim([triangleline[0,0],triangleline[0,1]])
ax.axis("off") #remove axis
ax.set_aspect(1) #aspect ratio of 1
axes[0].annotate("a",xy=(0,1),xycoords="axes fraction",fontSize=18,
fontWeight="bold")
axes[1].annotate("b",xy=(0,1),xycoords="axes fraction",fontSize=18,
fontWeight="bold")
fig.subplots_adjust(left=0.03,bottom=0.03,right=0.97,top=1.00)
plt.savefig("simplex.pdf",rasterized=True,dpi=400)
plt.show()

```

3.3 Figure 3

```

# -*- coding: utf-8 -*-
"""
@author: schenk

Poincare sections of a host-parasite system with 3 types
Replicator dynamics
Matching allele model (see u,v,w)

the poincare sections are only visible if many steps and many
generations are used
"""

from scipy.integrate import odeint
import matplotlib.pyplot as plt
import numpy as np

plt.close("all") # close figures
colours=['gold','limegreen','darkcyan','royalblue','indigo']

#=====
# Variables and settings
#=====

ks=np.array([1,3,5,10,23]) #k in ]0,25] defines initial kondition
u=-1. #payoff matrix entry alpha1
v=0. #payoff matrix entry alpha2
w=0. #payoff matrix entry alpha3
generations=50000.
steps=60000000.

```

```

=====
# Numerical integration and plot
=====

mh=np.array([[u,v,w],[w,u,v],[v,w,u]]) #payoff matrix for host
#generations=2 #to test the program
#steps=10 #to test the program
n=3 #number of hosts/parasites
mp=-np.transpose(mh) #payoff matrix for parasite with c=1
time = np.linspace(0.0,generations,steps) # start,end,steps
#figure for poincare section:
fig,axes=plt.subplots(nrows=1,ncols=2,figsize=(15.7,7.7))
#empty plotting for legend title:
axes[0].scatter([], [], color="white", marker='.',label="$h(0)$")

def deriv(y,t): #ode
h=y[:n]
p=y[n:]
h=h/sum(h) #normalisation
p=p/sum(p) #normalisation
dH=np.dot(mh,p) #fitness of host influenced by parasite f_H
bh=np.dot(dH,h) #average host fitness
hdot=h*(dH-bh) #ODE for hosts
bP=np.dot(mp,h) #fitness of parasite influenced by host f_P
dp=np.dot(bP,p) #average parasite fitness
pdot=p*(bP-dp) #ODE for parasites
return np.concatenate([hdot,pdot]) #ODEs

'''different initial conditions'''
p0=np.array([0.5,0.25,0.25]) #fixed initial cond. for parasites
counter=0 #counter for different initial conditions (colour)
for k in ks:
h0=np.array([0.5,0.01*k,0.5-0.01*k]) #different initial cond. for h
#numerical integration:
y = odeint(deriv,np.concatenate([h0,p0]),time)
h=y[:, :n] #host frequencies
p=y[:, n:] #parasite frequencies
#empty plotting for legend:
axes[0].scatter([], [], color=colours[counter], marker='.',
label='$($'+ '${:,.2f}$'.format(h0[0])+'$, $ '
+'${:,.2f}$'.format(h0[1])+'$, $ '
+'${:,.2f}$'.format(h0[2])+'$)$')

'''first conditon for poincare section'''
truth1=np.logical_and(-0.001<=h[1:,1]-h[1:,0]+p[1:,1]-p[1:,0],
0.001>=h[1:,1]-h[1:,0]+p[1:,1]-p[1:,0])
#only when going through poincare section from one side:
truth2=h[:-1,1]-h[:-1,0]+p[:-1,1]-p[:-1,0]>0.001
#combine both:

```



```

truth=np.append([False],np.logical_and(truth1,truth2))
hcond1=h[truth,:] #filter times for which condition holds
pcond1=p[truth,:]
axes[0].scatter(hcond1[:,0],pcond1[:,1],marker='.',
color=colours[counter],edgecolor='none',
rasterized=True) #plot

'''second condition for poincare section'''
truth1=np.logical_and(-0.001<=np.log(h[1:,0]*h[1:,1]*h[1:,2])
-np.log(p[1:,0]*p[1:,1]*p[1:,2]),
0.001>=np.log(h[1:,0]*h[1:,1]*h[1:,2])
-np.log(p[1:,0]*p[1:,1]*p[1:,2]))
#only when going through poincare section from one side:
truth2=np.log(h[:-1,0]*h[:-1,1]*h[:-1,2])
-np.log(p[:-1,0]*p[:-1,1]*p[:-1,2])<-0.001
#combine both:
truth=np.append([False],np.logical_and(truth1,truth2))
hcond2=h[truth,:]
pcond2=p[truth,:]
axes[1].scatter(hcond2[:,0],pcond2[:,1],marker='.',
color=colours[counter],edgecolor='none',
rasterized=True) #plot

counter+=1 #set counter higher for next initial condition

'''plot options'''
axes[0].legend(prop={'size':16},scatterpoints=1,
bbox_to_anchor=(1.05, 0.5), loc='center left',
borderaxespad=0.,markerscale=3) #set legend position
axes[0].annotate("a",fontsize=18,fontweight="bold",xy=(-0.1,1.1),
xycoords="axes fraction")
axes[1].annotate("b",fontsize=18,fontweight="bold",xy=(-0.1,1.1),
xycoords="axes fraction")
axes[0].set_xlabel('$h_1$',fontsize=18,family="sans-serif") #xlabel
axes[0].set_ylabel('$p_2$',fontsize=18,family="sans-serif") #ylabel
axes[0].set_xlim([0,0.8]) #xrange
axes[0].set_ylim([0,0.8]) #yrange
axes[0].set_aspect(1) #aspect ratio of plot
axes[0].annotate("$h_2-h_1+p_2-p_1=0$",ha="center",va="center",
fontsize=18,xy=(0.5,1.1),xycoords="axes fraction")
axes[1].set_xlabel('$h_1$',fontsize=18,family="sans-serif")
axes[1].set_ylabel('$p_2$',fontsize=18,family="sans-serif")
axes[1].set_xlim([0,0.8])
axes[1].set_ylim([0,0.8])
axes[1].set_aspect(1)
axes[1].annotate("$\log(h_0 \ h_1 \ h_2)-\log(p_0 \ p_1 \ p_2)=0$",
ha="center",va="center",fontsize=18,xy=(0.5,1.1),
xycoords="axes fraction")
fig.subplots_adjust(left=0.04,bottom=0.08,right=0.99,top=0.88,
wspace=0.62,hspace=0.04)

```

```
fig.savefig("poincare.pdf",rasterized=True,dpi=1200)  
plt.show()
```